Chapter 3

Evolution of F_L Structure Function at Small-x Using Regge Like Behaviour of Structure Function

In this chapter, the evolutions of longitudinal structure function F_L from its QCD evolution equation in next-to-leading order (NLO) at small-x is presented using the Regge like behaviour of the structure function. The proposed simple analytical expression for F_L structure function provides the t- and x-evolution equations to study the behaviour of F_L structure function at small-x. The calculated results are compared with the data of H1 [1–5], ZEUS [6] collaborations, results of Donnachie-Landshoff (DL) [7] model and theoretical predictions of MSTW08 [8], CT10 [9], ABM11 [10], NNPDF2.3 [11, 12] parameterizations. The comparison of our results with that of the results obtained by Boroun [13] is also studied here. We have also presented a comparative study of our predicted results with the results obtained in the previous chapter using Taylor expansion method. Our calculated results can be described within the framework of pQCD.

3.1 Theory

At small values of x ($x \leq 10^{-3}$), the QCD evolution equation for gluon dominating F_L^g structure function is given by [14]

$$\frac{\partial F_L^g(x,Q^2)}{\partial ln Q^2} = K_G(x,Q^2) \otimes F_L^g(x,Q^2). \tag{3.1}$$

Here $K_G(x,Q^2)$ is the gluon kernel known perturbatively up to the first few orders in $\alpha_s(Q^2)$. The symbol $\otimes$ represents the standard Mellin convolution. The kernel $K_G(x,Q^2)$ can be written as

$$K_G(x,Q^2) = \frac{\alpha_s(Q^2)}{4\pi}K_G^0(x) + \Big(\frac{\alpha_s(Q^2)}{4\pi}\Big)^2 K_G^1(x) \tag{3.2}$$

up to NLO, where $K_G^0(x)$ and $K_G^1(x)$ are the gluon splitting kernels in LO and NLO respectively. $K_G^0(x)$, $K_G^1(x)$ are given in ref. [15, 16] and their expressions are defined in Appendix A. Using all these and simplifying the QCD evolution equations for the F_L^g structure function in LO and NLO, we get

$$\frac{\partial F_L^g(x,t)}{\partial t} - \frac{\alpha_s(t)}{4\pi}\left[\frac{80}{9}\int_x^1 dw w^2(1-w)F_L^g\Big(\frac{x}{w},t\Big)\right] = 0 \tag{3.3}$$

and

$$\frac{\partial F_L^g(x,t)}{\partial t} - \frac{\alpha_s(t)}{4\pi}\left[\frac{80}{9}\int_x^1 dw w^2(1-w)F_L^g\Big(\frac{x}{w},t\Big)\right] - \Big(\frac{\alpha_s(t)}{4\pi}\Big)^2 I_1^G(x,t) = 0, \tag{3.4}$$

where

$$I_1^G(x,t) = \frac{160}{9}\int_x^1 dw f(w)F_L^g\Big(\frac{x}{w},t\Big). \tag{3.5}$$

Here $t = ln\frac{Q^2}{\Lambda^2}$, Λ is the QCD cut-off parameter and the function $f(w)$ is defined in Appendix A.

The strong coupling constant in higher order has the form [17]

$$\alpha_s(t) = \frac{4\pi}{\beta_0 t}\Big[1 - \frac{\beta_1}{\beta_0^2}\frac{lnt}{t} + O\Big(\frac{1}{t^2}\Big)\Big], \tag{3.6}$$

where β_0 and β_1 are the one loop and two loop corrections to the QCD β-function which are defined in chapter 2 (equations (2.10) and (2.11)).

Regge approach provides a very good description of the HERA data on the small-x behaviour of the structure function $F_2(x,Q^2)$ [18]. It explains the strong rise of the

structure function F_2 towards small values of x. This phenomenon is usually described with the help of the power like behaviour of the structure function at small-x as

$$F_2(x, Q^2) \propto x^{-\lambda},$$

where $\lambda > 0$. Here, the power λ is related with the intercept of the Reggeon contribution dominating at $x \to 0$, namely with the pomeron intercept, $\lambda = \alpha_p(0) - 1$. The small-$x$ behaviour of the structure function is mainly driven by the gluons in the proton and this gluon density is determined from the data on the slope $dF_2/dlnQ^2$ [19]. Thus, gluon density $G(x, Q^2)$ can be written as

$$G(x, Q^2) \sim \frac{dF_2}{dlnQ^2} \sim f(Q^2)x^{-\lambda_g},$$

where $f(Q^2)$ is a function of Q^2 and λ_g is the pomeron intercept minus one. The steep behaviour of the gluon distribution function generates a similar power like behaviour of F_2 structure function which can be expressed as $G(x, Q^2) \propto x^{-\lambda_g}$ [19]. The power of λ_g is found to be either $\lambda_g \simeq 0$ and $\lambda_g \simeq 0.5$ where the first one corresponds to soft pomeron and the second one to the hard (Lipatov) pomeron intercept [20]. As the longitudinal structure function is directly sensitive [21] to the gluon distribution function at small-x, we can use the same type of Regge behaviour to study the previous case.

Now, the Regge like behaviour of the longitudinal structure function can be expressed as

$$F_L^g(x, t) = f(t)x^{-\lambda_g}, \tag{3.7}$$

where $f(t)$ is a function of t, and λ_g is the pomeron intercept minus one. Now, $F_L^g\Big(\frac{x}{w}, t\Big)$ can be written as

$$F_L^g\Big(\frac{x}{w}, t\Big) = F_L^g(x, t)w^{\lambda_g}. \tag{3.8}$$

Using equations (3.7), (3.8) and leading order term of equation (3.6) in equation (3.3)

we get

$$\frac{\partial F_L^g(x,t)}{\partial t} = \frac{F_L^g(x,t)}{t} P(x) \tag{3.9}$$

with

$$P(x) = \frac{80}{9\beta_0} \int_x^1 dw(1-w)w^{2+\lambda_g}.$$

Integrating equation (3.9) we get

$$F_L^g(x,t) = Ct^{P(x)}, \tag{3.10}$$

where C is a constant of integration.

Applying initial conditions at $t = t_0$, $F_L(x,t) = F_L(x,t_0)$ and at $x = x_0$, $F_L(x,t) = F_L(x_0,t)$, the t and x-evolutions for F_L^g structure function in LO can be written as

$$F_L^g(x,t) = F_L^g(x,t_0)\Big(\frac{t}{t_0}\Big)^{P(x)} \tag{3.11}$$

and

$$F_L^g(x,t) = F_L^g(x_0,t)t^{[P(x)-P(x_0)]} \tag{3.12}$$

respectively. Here $F_L^g(x,t_0)$ and $F_L^g(x_0,t)$ are defined in chapter 2.

Proceeding in the similar manner from equation (3.4), we obtain the t- and x-evolutions for F_L^g structure function in NLO as

$$F_L^g(x,t) = F_L^g(x,t_0)\frac{t^{(1+\frac{b}{t})P_1(x)}}{t_0^{(1+\frac{b}{t_0})P_1(x)}} exp\Big[b\Big(\frac{1}{t}-\frac{1}{t_0}\Big)P_1(x)\Big] \tag{3.13}$$

and

$$F_L^g(x,t) = F_L^g(x_0,t)t^{(1+\frac{b}{t})[P_1(x)-P_1(x_0)]} exp\Big[\frac{b}{t}(P_1(x)-P_1(x_0))\Big] \tag{3.14}$$

respectively, where

$$P_1(x) = \frac{1}{\beta_0}[P(x) + T_0Q(x)] \qquad \text{and} \qquad Q(x) = \frac{160}{9}\int_x^1 dw w^{\lambda_g} f(w).$$

The numerical parameter T_0 is calculated for the particular range of Q^2 under study as described in ref. [22]. Here we have considered the values of $T_0 = 0.0278$ within the range $1.5 \leq Q^2 \leq 800GeV^2$ as described in chapter 2.

Thus we have obtained the analytical expressions for the t- and x-evolutions of longitudinal structure function F_L^g as the solution of its evolution equation. Equations (3.11), (3.13) and (3.12), (3.14) finally give us the t-evolutions and x-evolutions of F_L^g structure function in LO and NLO respectively.

3.2 Results and Discussions

In this chapter, we have calculated the t- and x-evolutions of the gluon dominating longitudinal structure function F_L^g at small-x in leading and next-to-leading orders using the Regge like behaviour of the structure function. The obtained results are compared with the available H1 [1–5] and ZEUS experimental data [6], results of the Donnachie-Landshoff (DL) model [7] and the theoretical predictions from MSTW08 [8], CT10 [9], ABM11 [10], NNPDF2.3 [11, 12] parameterizations at several x and Q^2 values. The kinematical ranges for H1 2001, H1 2007, H1 2011, H1 2014 and ZEUS 2009 data, are $1.5 \leq Q^2 \leq 150GeV^2$ and $3 \times 10^{-5} \leq x \leq 0.2$, $2.5 \leq Q^2 \leq 25GeV^2$ and $5 \times 10^{-5} \leq x \leq 0.12$, $1.5 \leq Q^2 \leq 120GeV^2$ and $2.9 \times 10^{-5} \leq x \leq 0.01$, $35 \leq Q^2 \leq 800GeV^2$ and $6.5 \times 10^{-4} \leq x \leq 0.65$ and $20 < Q^2 < 130GeV^2$ and $5 \times 10^{-4} < x < 0.07$ respectively.

The t- and x-evolution results of F_L^g structure function are depicted in figure 3.1 to figure 3.6, where we have compared our results with related experimental data and fit. Here, the longitudinal structure function, measured in the range $5 \leq Q^2 \leq 800GeV^2$ and $10^{-4} \leq x \leq 10^{-1}$, have been used for our analysis. The value of y used is ≥ 0.5, as from this value onwards the contribution of F_L^g structure function is significant towards the total cross section [23]. Here the value of gluon distribution function exponent λ_g is taken as 0.5 as in the region of small-x this value describes the HERA data well [24, 25]. In figure 3.1, $F_L^g(x, Q^2)$ structure function results are plotted against

Q^2 for different values of x in comparison with the H1, ZEUS data and results of DL model. In figures 3.2 to 3.6, $F_L^g(x, Q^2)$ structure function is plotted against x for different values of Q^2 in comparison with the H1, ZEUS data, the results of DL model and the theoretical predictions of F_L using standard gluon distribution function by MSTW08, CT10, ABM11 and NNPDF2.3 parameterizations. Here the vertical error bars are both statistical and systematic errors for both H1 and ZEUS data. To show that in spite of large uncertainty of the experimental data, our results lie within the framework of pQCD we have compared our results with the model fit and parameterizations. In case of the x-evolution results described in figure 3.2 to figure 3.6, the behaviour of LO, NLO curves are not exactly the same as we have considered the input point from different parameterizations. The behaviour of LO and NLO curves in both the t- and x-evolutions of F_L^g structure function are different (i.e., sometimes NLO results overestimate LO prediction and vice versa) and this behaviour of the curves depend only on the the expressions used for calculation of the structure function. Moreover, with reference to some recent papers [26–29], we can say that the behaviour of the LO, NLO curves depend only on the applied method.

It is observed from the t-evolution graphs in figure 3.1 that, our result shows almost similar behaviour with that of H1 and ZEUS data. To indicate that in spite of large uncertainty in experimental data we have compared our results with the results of DL model which also shows good agreement with results of model. Here the Q^2-dependence behaviour of structure function shows slight increasing behaviour with respect to Q^2. This is due to the presence of evolution kernel in the final expression for t-evolution of F_L^g structure function. In case of the plot $x = 0.0004$, we have used the input point from DL model to study the evolution of F_L structure function. As the input point is near the end of the error bar of F_L data and our evolution of structure function shows slightly increasing behaviour, so in this case our calculated results at some point are outside the error bars. Among all the plots, the plot at $x = 0.002$ shows better

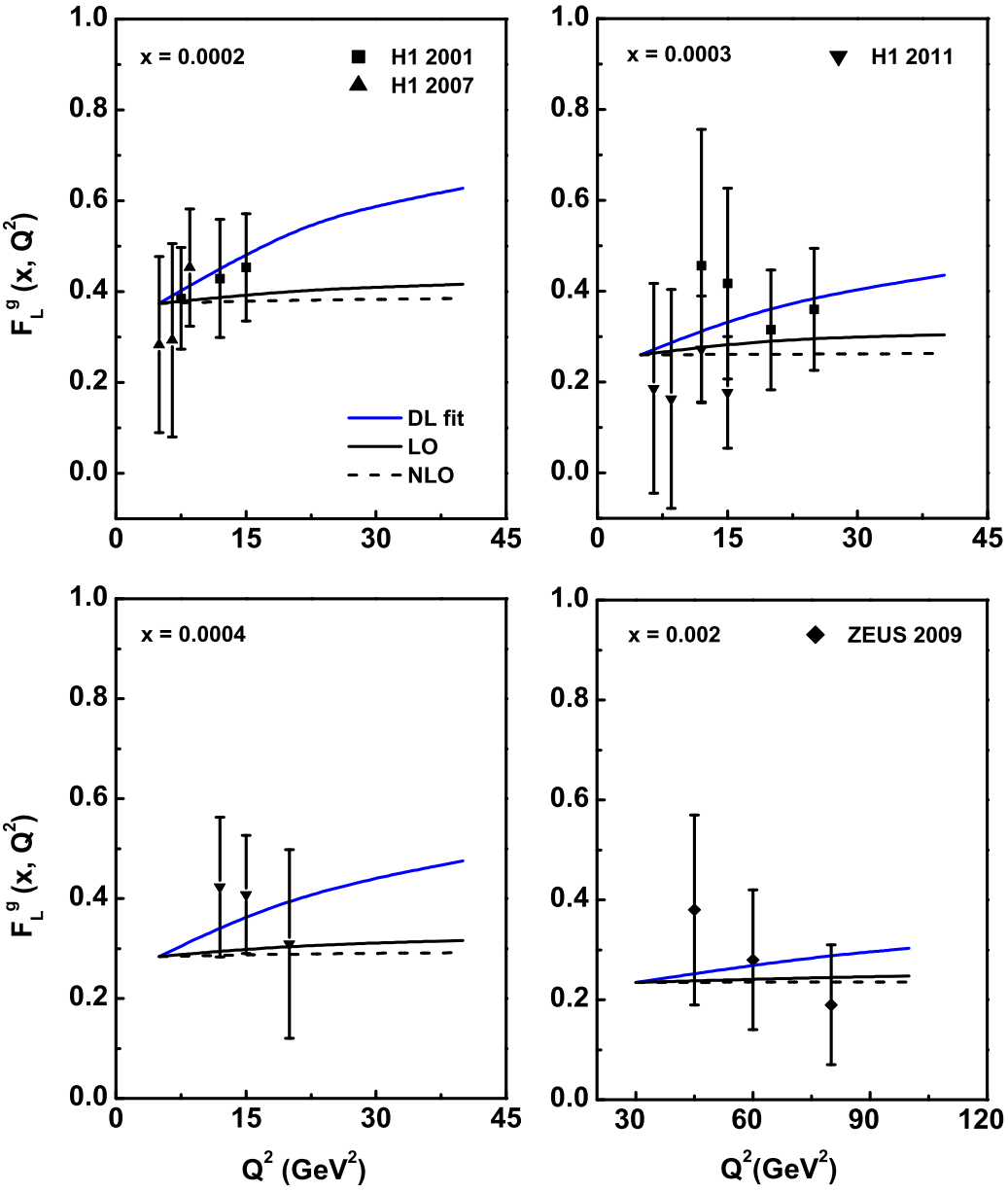

Figure 3.1: t-evolution results of F_L^g structure function up to NLO using Regge theory in comparison with the H1, ZEUS data and results of DL model.

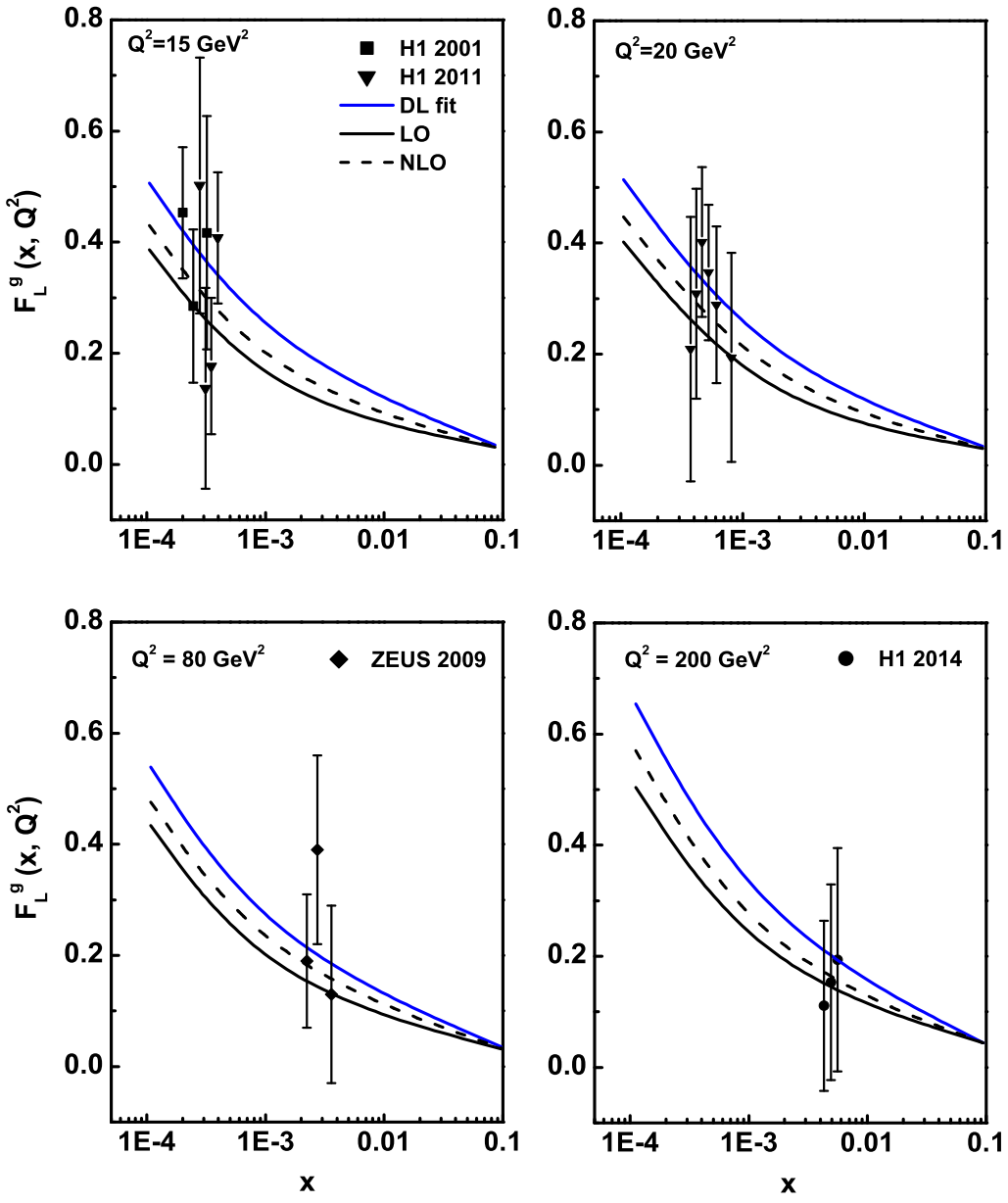

Figure 3.2: x-evolution results of F_L^g structure function up to NLO using Regge theory in comparison with the H1, ZEUS data and results of DL model.

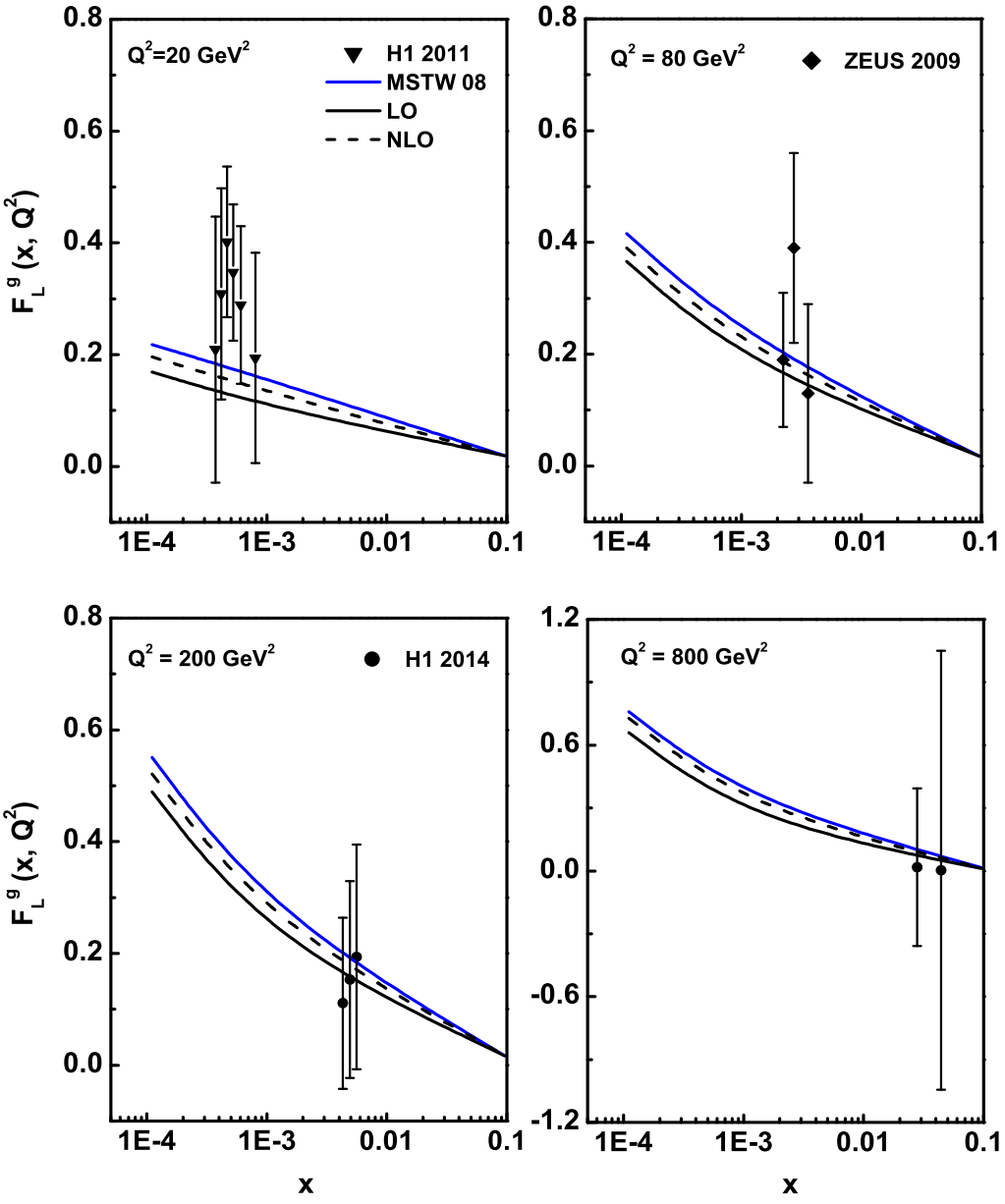

Figure 3.3: x-evolution results of F_L^g structure function up to NLO using Regge theory in comparison with the H1, ZEUS data and the theoretical prediction of MSTW08.

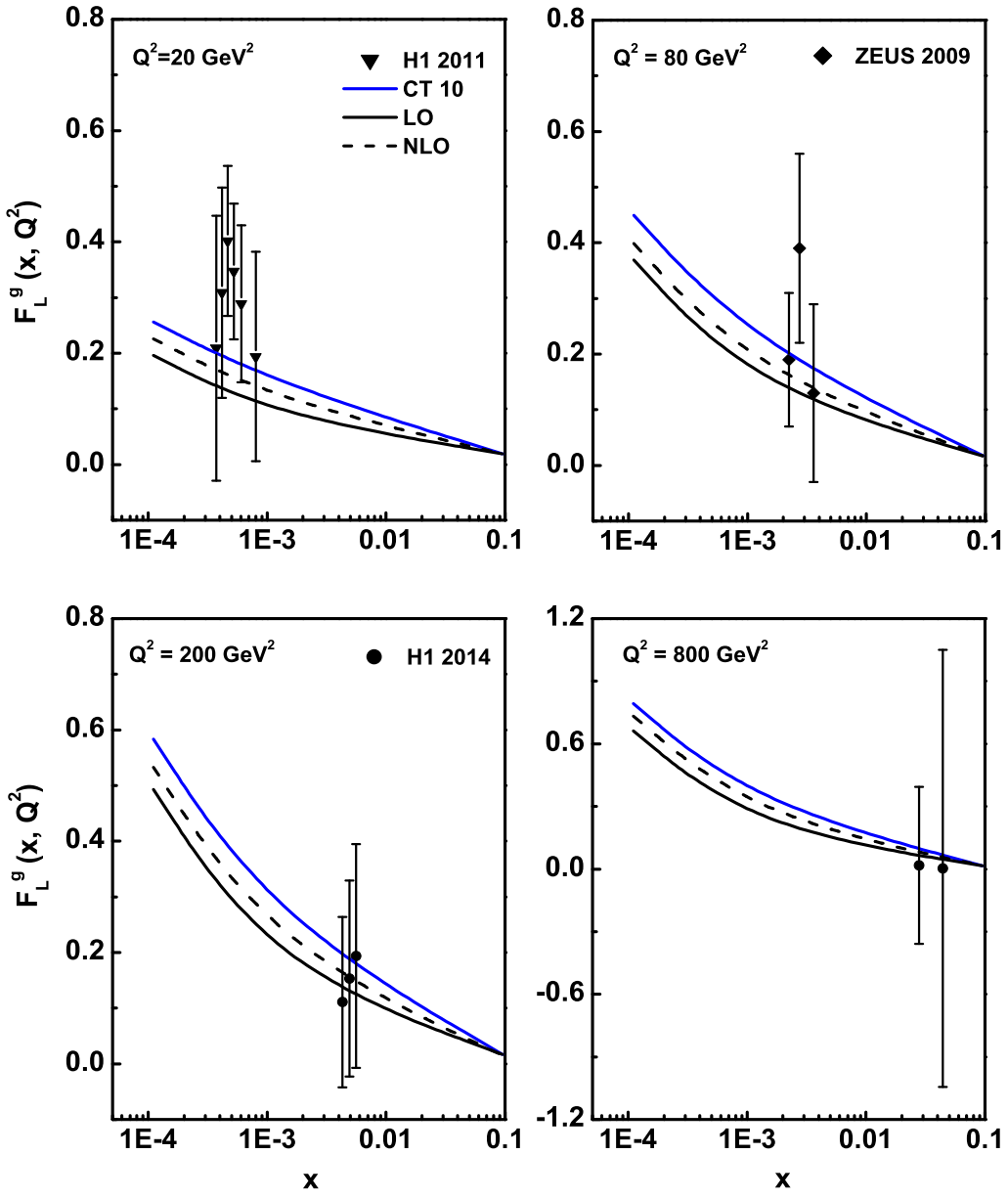

Figure 3.4: x-evolution results of F_L^g structure function up to NLO using Regge theory in comparison with the H1, ZEUS data and the theoretical prediction of CT10.

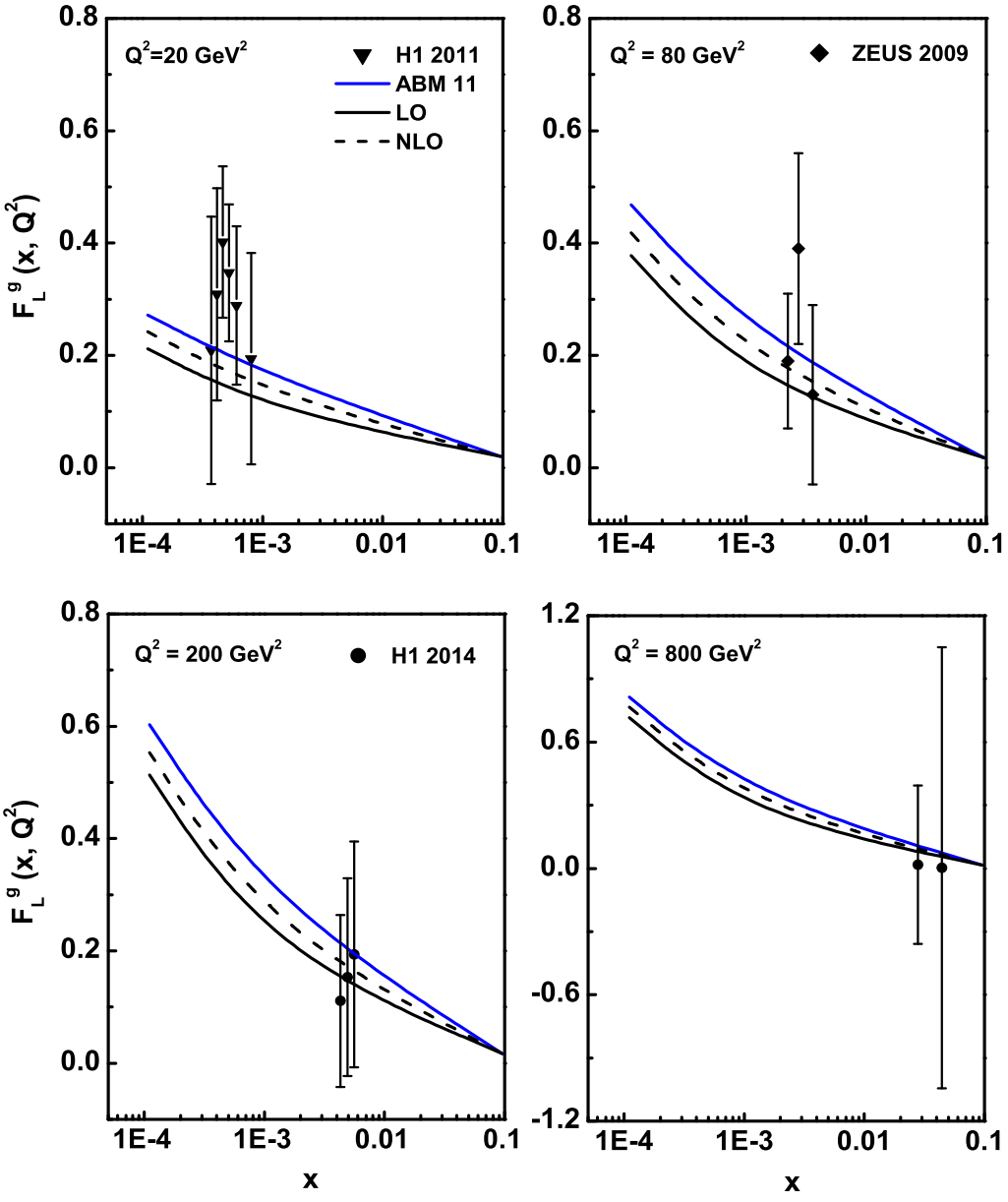

Figure 3.5: x-evolution results of F_L^g structure function up to NLO using Regge theory in comparison with the H1, ZEUS data and the theoretical prediction of ABM11.

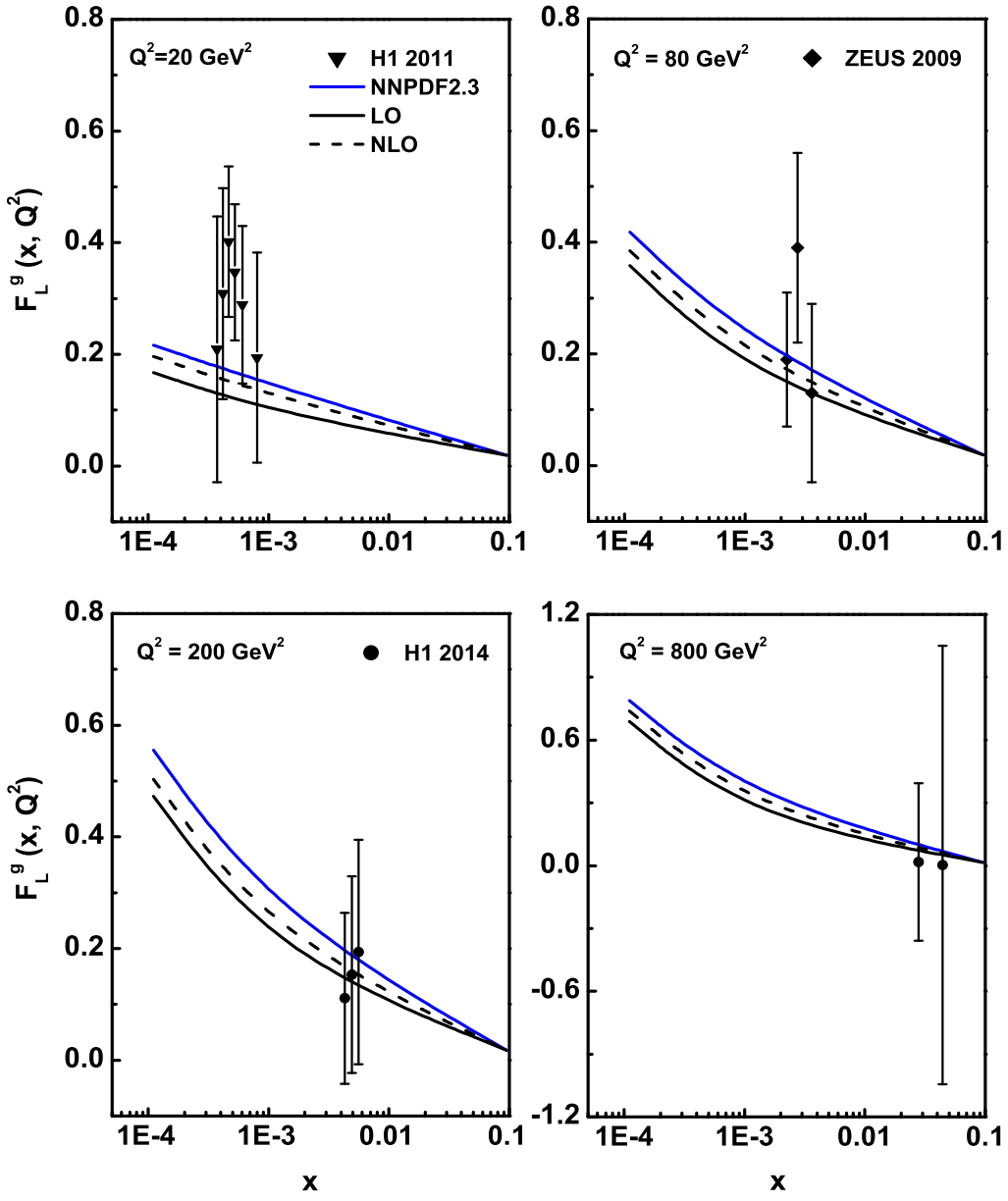

Figure 3.6: x-evolution results of F_L^g structure function up to NLO using Regge theory in comparison with the H1, ZEUS data and the theoretical prediction of NNPDF2.3.

agreement with the model fit i.e., the Q^2 dependence of structure function obtained by our approach shows better agreement with the results of model fit for this x value. In all the cases, our calculated F_L structure function in LO and NLO increase with the values of Q^2 in the given range like the results of DL models. This is an expected result from QCD also. At small-x, F_L increases with Q^2 as we resolve increasing numbers of soft partons with increasing Q^2 [30]. From the x-evolution graphs, it is observed that our result shows good agreement with those of H1, ZEUS data and those predicted by model and parameterizations. Also it is observed that compatibility with data becomes better with increasing values of Q^2.

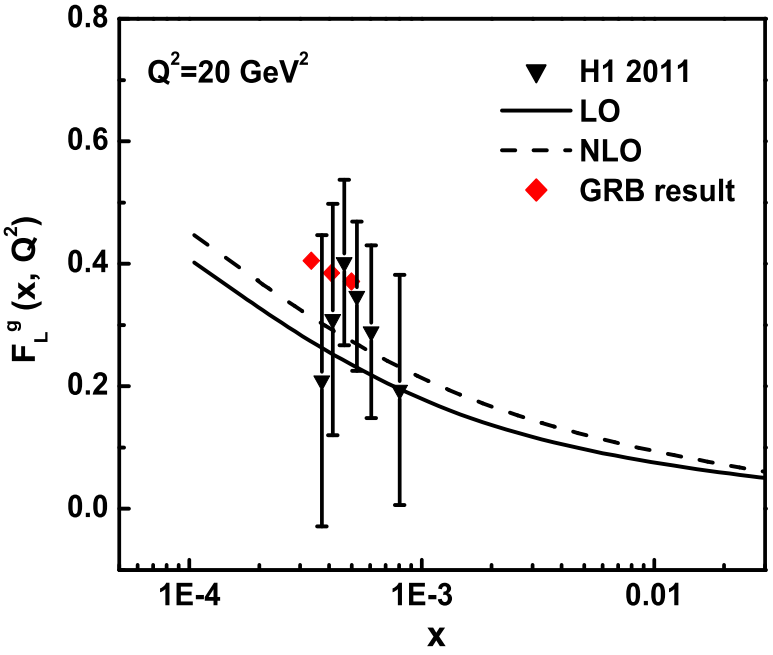

Figure 3.7: x-evolution results of F_L^g structure function up to NLO using Regge theory in comparison with the H1 data and the theoretical prediction of Boroun (GRB) [13].

We have also compared our x-evolution results with the results obtained by Boroun

[13] which is shown in figure 3.7. Here they have reported an analytical expression to determine the F_L structure function in NLO at small-x. In their approach Regge like behaviour of gluon distribution function is used which reflects good agreement of their results with recent data and fit. As depicted in figure 3.7 our result shows similar behaviour with the results in ref. [13]. In both the cases, the structure function increases towards small values of x as expected from QCD. Both the results does not show exactly the same behaviour as the methods for calculation of the structure function in both the cases are different.

3.2.1 Comparative study of our results predicted by Regge theory and Taylor expansion method

Here we have presented a comparative analysis of our results predicted by Regge theory (RT) approach and results of chapter 2 i.e., obtained by Taylor expansion (TE) method. Figures 3.8 to 3.13 show the comparison of the evolutions of F_L^g structure functions obtained by the two methods already discussed above.

The comparison of our results of the t-evolution of F_L^g structure function at small-x is presented in figure 3.8 which reflects similar nature with the results of DL model in spite of the large uncertainties of the data. The results predicted by Taylor expansion method shows better agreement with the results of the model than those obtained by the Regge theory approach. This implies that the compatibility of the t-evolution results with the model fit and data depends on the expression of evolution kernel of F_L. Due to the presence of evolution kernel in the final expression for t-evolution of F_L^g structure function in equations (3.11) and (3.13) in Reege theory approach, the growth of structure function is not sharp as that obtained by the Taylor expansion method where the final expressions for determination of t-evolution of structure function, equations (2.21) and (2.23) are independent of evolution kernel.

Figures 3.9 to 3.13 describe the comparison of the behaviour of F_L^g structure function

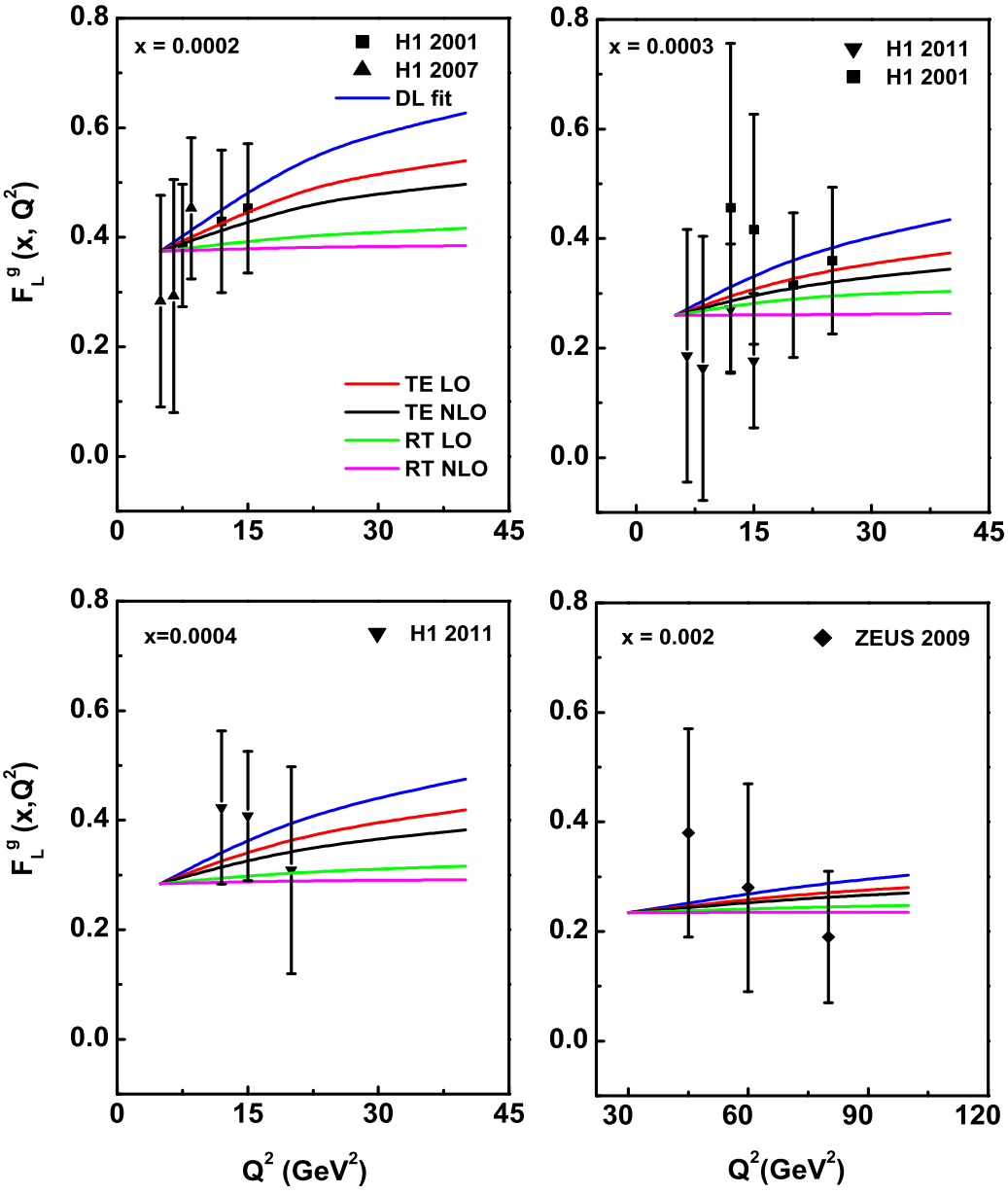

Figure 3.8: Comparison of t-evolution results of F_L^g structure function predicted by Regge theory approach and Taylor expansion method and DL model.

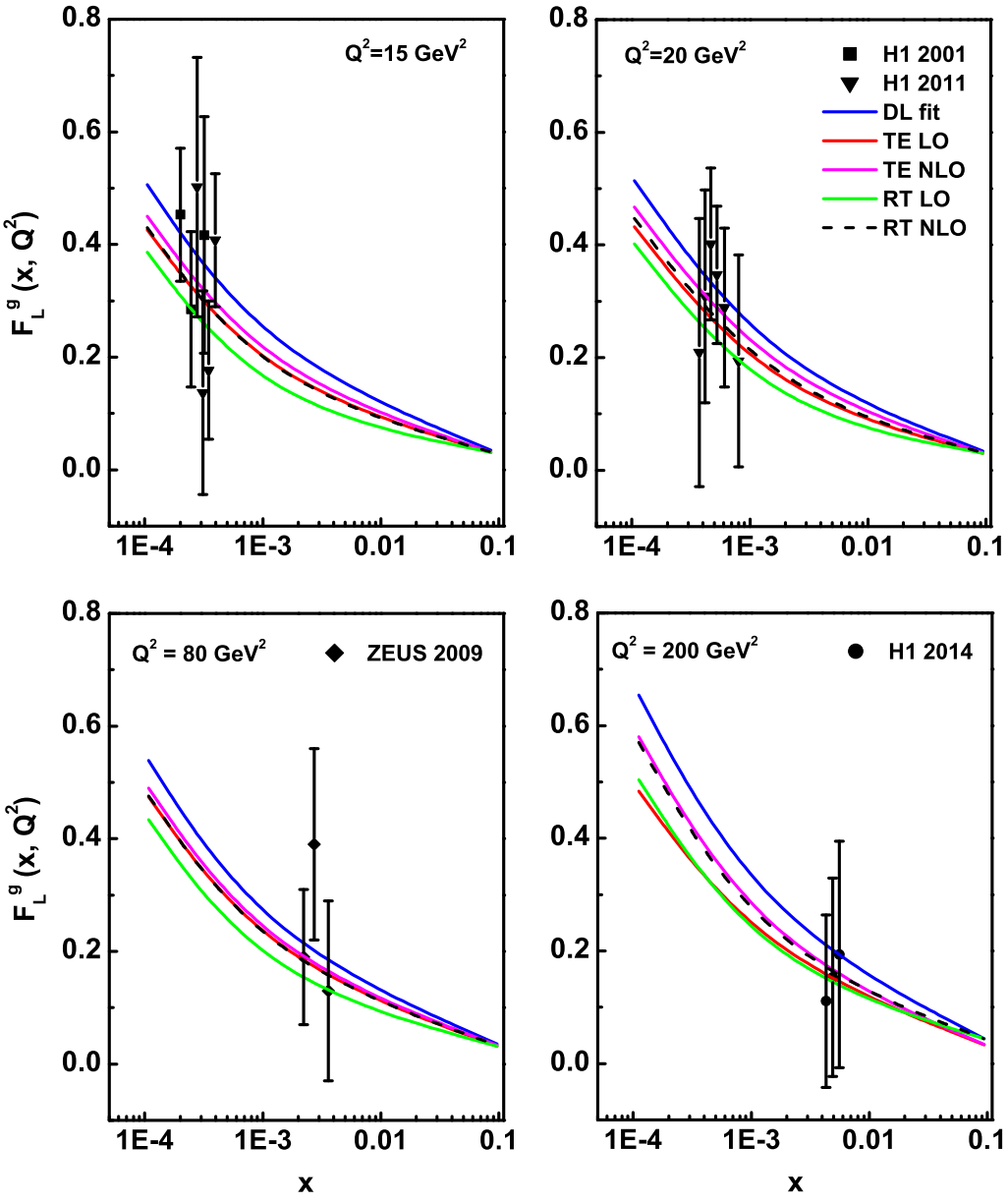

Figure 3.9: Comparison of x-evolution results of F_L^g structure function predicted by Regge theory approach and Taylor expansion method and DL model.

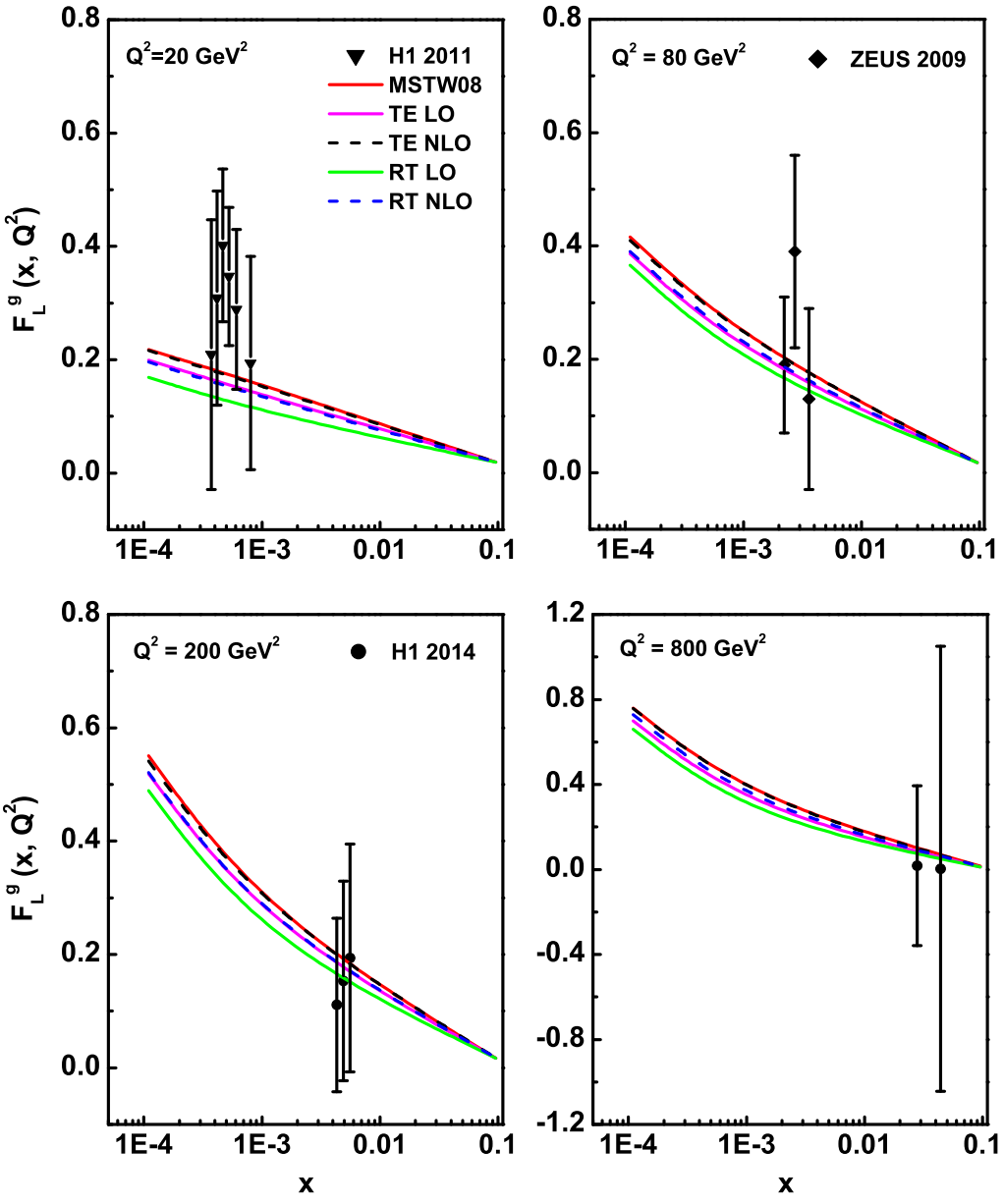

Figure 3.10: Comparison of x-evolution results of F_L^g structure function predicted by Regge theory approach and Taylor expansion method and MSTW08.

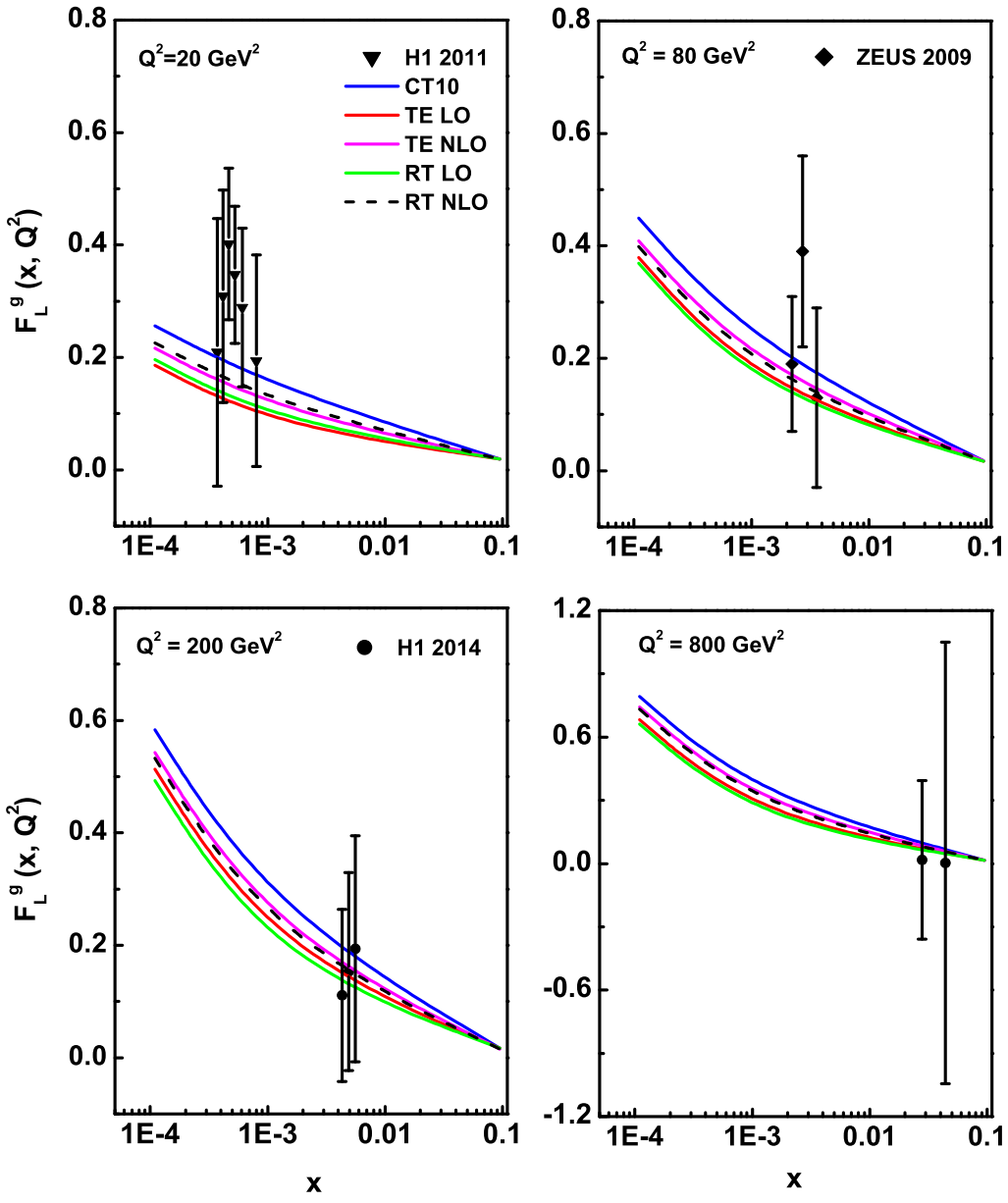

Figure 3.11: Comparison of x-evolution results of F_L^g structure function predicted by Regge theory approach and Taylor expansion method and CT10.

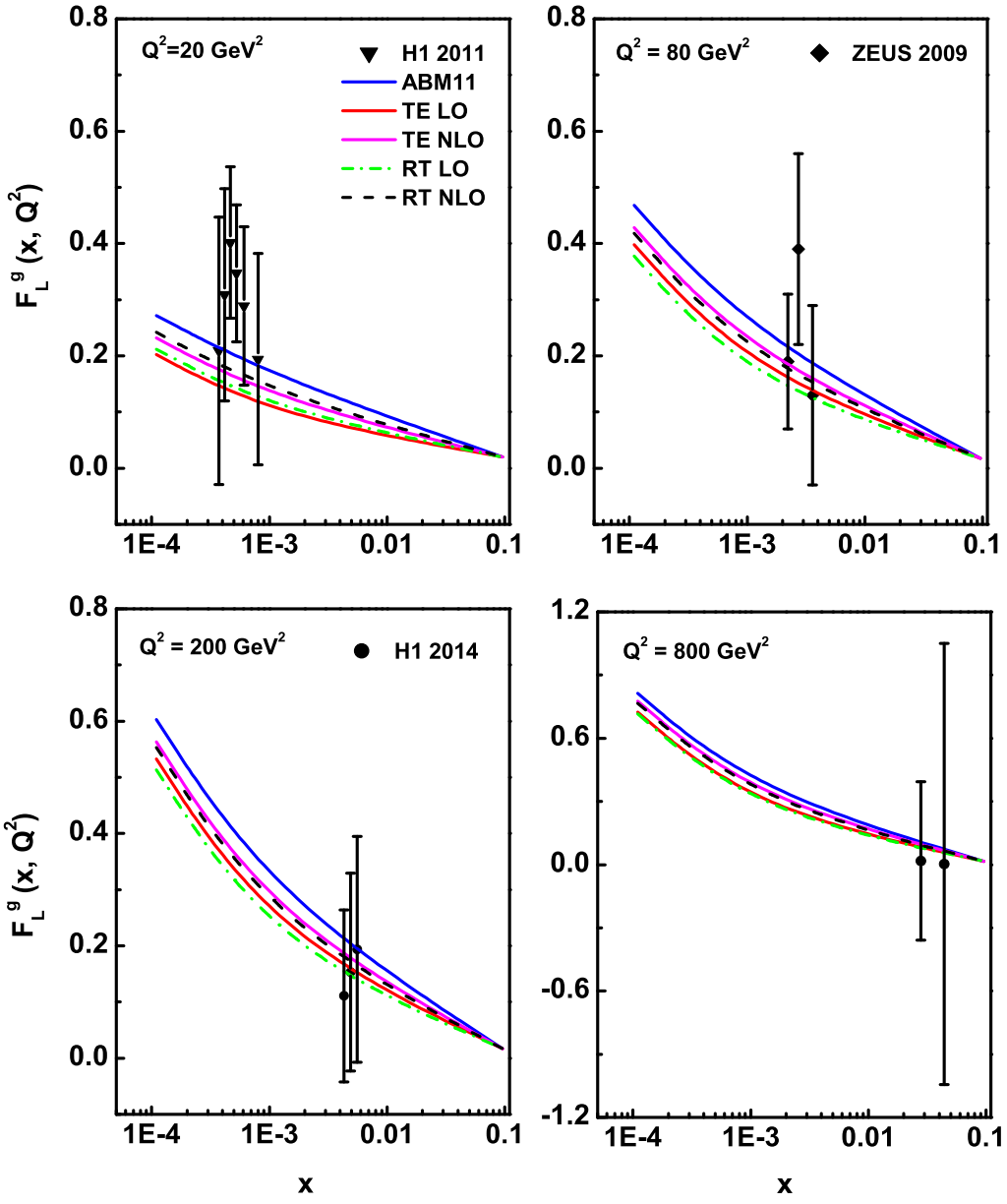

Figure 3.12: Comparison of x-evolution results of F_L^g structure function predicted by Regge theory approach and Taylor expansion method and ABM11.

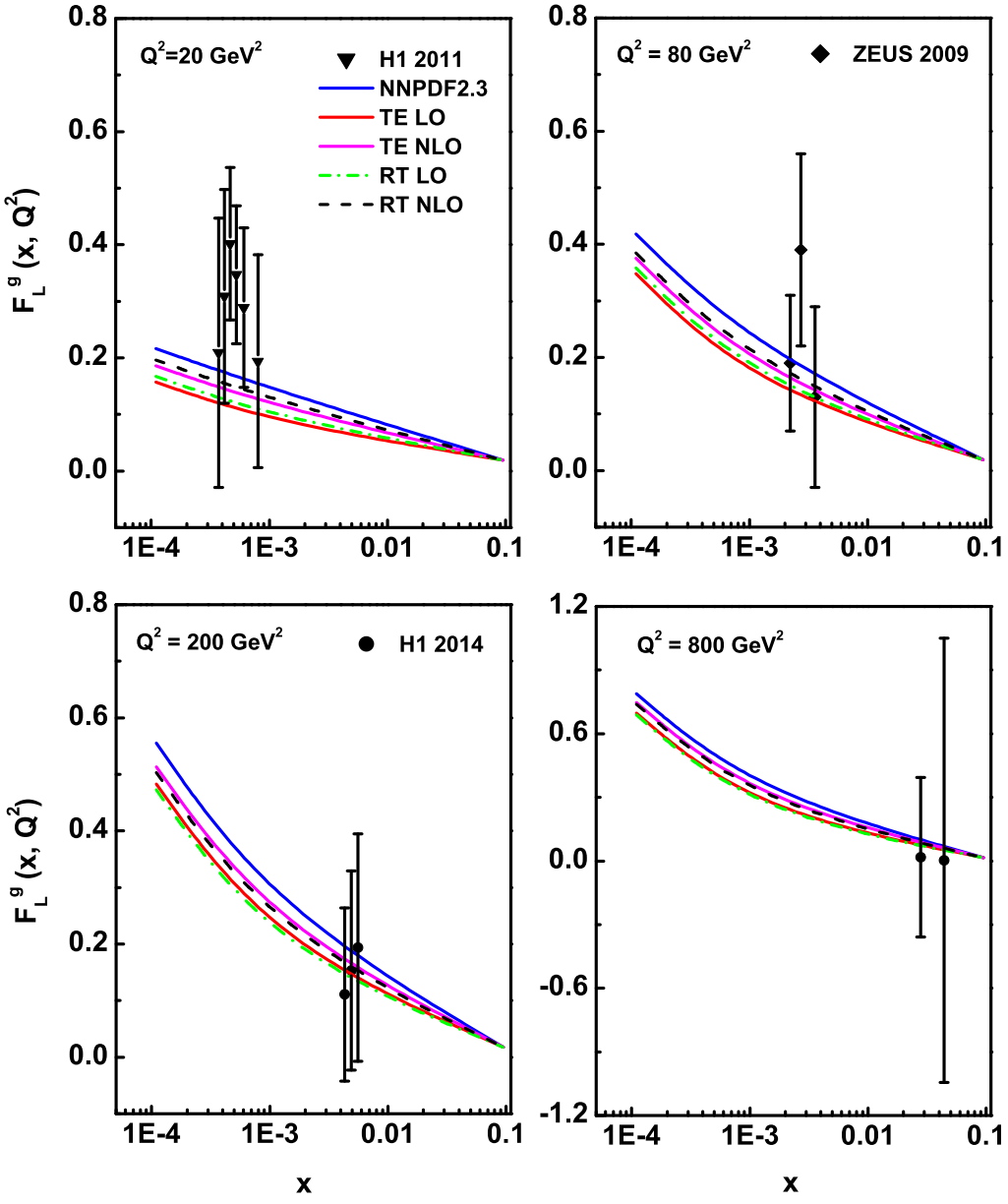

Figure 3.13: Comparison of x-evolution results of F_L^g structure function predicted by Regge theory approach and Taylor expansion method and NNPDF2.3.

with respect to x which shows good agreement with the data, model fit and parameterizations. In all the graphs, F_L^g structure function predicted by both approach increases towards small values of x. Though the results of obtained by TE approach are slightly higher than those of RT approach in almost all the cases, yet both the methods can be applied to calculate the F_L^g structure function at small-x.

3.3 Conclusions

In this chapter, we have obtained an analytical solution of evolution equation for longitudinal structure function F_L^g up to NLO using the Regge like behaviour of the structure function. Here, we have studied the behaviour of the t and x-evolutions of F_L^g structure function up to NLO only. Due to the unavailability of the evolution kernel at NNLO we are unable to calculate the same at this order. We have compared our results with the recent experimental data to confirm the validity of our calculations. The variation of F_L^g structure function with x and Q^2 shows similar nature with the experimental data as well as the model fit and parameterizations which shows the compatibility of Regge behaviour with the perturbative evolution of structure function at small-x. At small-x, our results show that the longitudinal structure function F_L^g increases as the values of Q^2 increases and x decreases. The increasing behaviour of F_L^g structure function in this approach follows the power law behaviour of structure function as predicted by Regge theory. As in our given range of x, we have considered only the gluon dominating part of the structure function, so we can say that the gluon contribution to the longitudinal structure function increases as the values of Q^2 increases and x decreases. From the comparative study of evolution of F_L structure function predicted by Regge theory approach and Taylor expansion method shows that results obtained by both the method are in good agreement with data and parameterizations.

References

[1] Aaron, F. D., et al. Measurement of the inclusive $e^{\pm}p$ scattering cross section at high inelasticity y and of the structure function F_L, *Eur. Phys. J. C.* **71** (3), 1579-1–50, 2011.

[2] Adloff, C., et al. Deep-inelastic inclusive ep scattering at low x and a determination of α_s, *Eur. Phys. J. C.* **21** (1), 33–61, 2001.

[3] Pardos, C. D. *Studies for the direct measurement of the proton structure function F_L with the H1 detector at HERA*, Ph.D. thesis, DESY, Zeuthen, Germany, 2007.

[4] Piec, S. *Measurement of the Proton Structure Function F_L with the H1 Detector at HERA*, Ph.D. thesis, Humboldt University of Berlin, Germany, 2009.

[5] Andreev, V., et al. Measurement of Inclusive ep Cross Sections at High Q^2 at $\sqrt{s} = 225$ and $252GeV$ and of the Longitudinal Proton Structure Function F_L at HERA, *Eur. Phys. J. C* **74** (4), 2814-1–26, 2014.

[6] Chekanov, S., et al. Measurement of the longitudinal proton structure function at HERA, *Phys. Lett. B* **682** (1), 8–22, 2009.

[7] Donnachie, A. and Landshoff, P. V. The protons gluon distribution, *Phys. Lett. B* **550** (3-4), 160–165, 2002.

[8] Martin, A. D., et al. Parton distributions for the LHC, *Eur. Phys. J. C* **63** (2), 189–285, 2009.

[9] Hung-Liang, Lai., et al. New parton distributions for collider physics, *Phys. Rev. D* **82** (7), 074024-1–24, 2010.

[10] Alekhin, S., Blemlein, J. and Moch, S. The ABM parton distributions tuned to LHC data, *Phys. Rev. D* **89** (5), 054028-1–21, 2014.

[11] Ball, R. D., et al. Parton distributions with LHC data, *Nucl. Phys. B* **867** (2), 244–289, 2013.

[12] Forte, S., et al. Heavy quarks in deep-inelastic scattering, *Nucl. Phys. B* **834** (1-2), 116–162, 2010.

[13] Boroun, G. R. Hard-pomeron behavior of the longitudinal structure function F_L in the next-to-leading order at low x, *Int. J. Mod. Phys. E* **18** (1), 131–140, 2009.

[14] Moch, S. and Vogt, A. Threshold resummation of the structure function F_L, *J. High Energy Phys.* **2009** (04), 081-1–11, 2009.

[15] Kazakov, D. I., et al. Complete Quartic α_s^2 correction to the deep-inelastic longitudinal structure function F_L in QCD, *Phys. Rev. Lett.* **65** (13), 1535–1538, 1990.

[16] Guillen, J. S., et al. Next-to-leading order analysis of the deep inelastic $R = \sigma_L/\sigma_T$, *Nucl. Phys. B* **353** (2) 337–345, 1991.

[17] Abbott, L. F., Atwood, W. B. and Barnett, R. M. Quantum-chromodynamic analysis of eN deep-inelastic scattering data, *Phys. Rev. D* **22** (3), 582–593, 1980.

[18] Donnachie, A. and Landshoff, P. V. Small x: two pomerons, *Phys. Lett. B* **437** (3-4), 408–416 , 1998.

[19] Kotikov, A. V. and Parente, G. The gluon distribution as a function of F_2 and $dF_2/dlnQ^2$ at small x. The next-to-leading analysis, *Phys. Lett. B* **379** (1-4), 195–201, 1996.

[20] Donnachie, A. and Landshoff, P. V. Perturbative QCD and Regge theory: closing the circle, *Phys. Lett. B* **533** (3-4), 277–284 , 2002.

[21] Cooper-Sarkar, A. M., et al. Measurement of the longitudinal structure function and the small x gluon density of the proton, *Z. Phys. C* **39** (2), 281–290, 1988.

[22] Baishya, R. and Sarma, J. K. Semi numerical solution of non-singlet DokshitzerGribovLipatovAltarelliParisi evolution equation up to next-to-next-to-leading order at small x, *Eur. Phys. J. C* **60** (4), 585–591, 2009.

[23] Glazov, S. Measurement of DIS Cross Section at HERA, *Braz. J. Phys.* **37** (2C), 793–797, 2007.

[24] Jamil, U. and Sarma, J. K. Regge behaviour of distribution functions and evolution of gluon distribution function in next-to-leading order at low-x, *Pramana J. Phys.* **71** (3), 509–519, 2008.

[25] Martin, A. D., Ryskin, M. G. and Watt, G. Simultaneous QCD analysis of diffractive and inclusive deep-inelastic scattering data, *Phys. Rev. D* **70** (9), 091502-1–5, 2004.

[26] Rezaei, B. and Boroun, G. R. Analytical solution of the longitudinal structure function F_L in the leading and next-to-leading-order analysis at low x with respect to Laguerre polynomials method, *Nucl. Phys. A* **857** (1), 42–47, 2011.

[27] Nematollahi, H., Yazdanpanah, M. M. and Mirjalili, A. NNLO longitudinal proton structure function, based on the modified χQM, *Mod. Phys. Lett. A* **27** (31),1250179-1-11 ,2012.

[28] Boroun, G. R. and Rezaei, B. Analysis of the proton longitudinal structure function from the gluon distribution function, *Eur. Phys. J. C* **72** (11), 2221-1-5, 2012.

[29] Devee, M., Baishya, R. and Sarma, J. K. Evolution of singlet structure functions from DGLAP equation at next-to-next-to-leading order at small-x, *Eur. Phys. J. C* **72** (6), 2036-1-11, 2012.

[30] Kwiecinski, J., et al. Parton distributions at small x, *Phys. Rev. D* **42** (11), 3645–3659, 1990. □